Annals of Clinical and Medical Case Reports

Research Article ISSN 2639-8109 | Volume 6

"On the Detection of cTnI - A Comparison of Surface-Plasmon Optical -, Electrochemical -, and Electronic Sensing Concepts"

Rodrigues T[1,2], Mishyn V[1,2], Bozdogan A[1,3], Leroux, Y.R.[4], Happy H[2], Kasry A[3,5], Boukherroub R[2], Dostalek J[1], Aspermair P[1], Bintinger J[1,6], Kleber C[6], Szunerits S[2] and Knoll W[1,3,6]

[1]AIT Austrian Institute of Technology GmbH, Biosensor Technologies, 3430 Tulln, Austria

[2]Univ. Lille, CNRS, Centrale Lille, Univ. Polytechnique Hauts-de-France, UMR 8520 - IEMN, F-59000 Lille, France

[3]CEST Competence Centre for Electrochemical Surface Technology, 2700 Wiener Neustadt, Austria

[4]Univ. Rennes, CNRS, ISCR –UMR 6226, Campus de Beaulieu, F-35000 Rennes, France

[5]Nanotechnology Research Centre (NTRC), The British University in Egypt (BUE), El-Sherouk City, Suez Desert Road, Cairo 11837, Egypt

[6]Department of Physics and Chemistry of Materials, Faculty of Medicine/Dental Medicine, Danube Private University, Krems, Austria

***Corresponding author:**

Wolfgang Knoll,
AIT Austrian Institute of Technology,
Tel+43 664 2351720, +4350550 4000,
E-Mail: wolfgang.knoll@ait.ac.at

Keywords:

Cardiac Troponin I; Biosensor; Surface-Plasmon Fluorescence Spectroscopy; Differential Pulse Voltammetry; Graphene Field-Effect Transistor

Received: 12 Feb 2021
Accepted: 01 Mar 2021
Published: 06 Mar 2021

Citation:

Knoll W. "On the Detection of cTnI - A Comparison of Surface-Plasmon Optical -, Electrochemical -, and Electronic Sensing Concepts". Ann Clin Med Case Rep. 2021; V6(2): 1-16

1. Introduction

"Cardiovascular diseases (CVDs) are the number one cause of death globally, taking an estimated 17.9 million lives each year. CVDs are a group of disorders of the heart and blood vessels and include coronary heart disease, cerebrovascular disease, rheumatic heart disease, and other conditions. Four out of five CVD deaths are due to heart attacks and strokes, and one third of these deaths occurs prematurely in people under 70 years of age" (cited from [1]). In addition, the total economic burden of CVD is enormous; the costs are expected to rise from approximately US$ 863 billion in 2010 to a staggering US$ 1,044 billion by 2030 worldwide [2].

Acute Myocardial Infarction (AMI), the most life-threatening version of acute coronary syndromes, causes severe irreversible tissue injury in the myocardium. The analysis of AMI primarily depends on electrocardiography (ECG) but only 57% of patients can be diagnosed correctly for AMI, and some of these patients can even show normal or non-diagnostic ECG when presented to the Emergency Room [3]. What is worse, 25% of AMI have happened without any symptoms like pain in the chest, back, or jaw. Therefore, a rapid, sensitive, and cost-efficient platform is needed to meet the diagnostic requirements in AMI detection [4].

Over the years, various marker molecules have been proposed for AMI diagnostics, among which were Aspartate Transaminase, Creatine Kinase, or Myoglobin [5]; although cardiac Troponin T (cTnT) or Troponin I (cTnI) have become the golden standards for myocardial infarction diagnostics and resulted in the development of the first bedside testing method [6]. During these years, there have been significant improvements in assays for cTn with regards to analytical sensitivity and precision at low concentrations [7]. The first-generation assay was not able to detect low plasma concentrations of troponin, while the second generation could identify injury earlier, but was not sensitive enough for healthy people. Finally, the third generation are high-sensitivity troponin assays and can reliably detect the low troponin levels in healthy individuals, as well as can differentiate patients with myocardial ischemia onset and early necrosis [8].

The corresponding cut off levels of cTnI in plasma for healthy patients were in the first generation 0.5 ng mL^{-1} (500 pg mL^{-1}). With

the advances in the development of high sensitivity troponin tests, the reference cutoff levels for cTnI in serum used to establish AMI has been progressively lowered and is currently in the range of 26 pg mL^{-1} [9]. This is about 100-1000 times lower than the cTnI level in patients with a clear positive test for AMI, with serum levels of cTnI as high as 5-50 ng mL^{-1} [10]. Upon the occurrence of an AMI, the death of cardiac myocytes causes the cTnI concentration up to 50 ng mL^{-1} within 3−6 h, and finally to a level around 550 ng mL^{-1} where it remains elevated for a few days, while that of other biomarkers will decline more rapidly [11].

The enormous clinical importance of having reliable methods and devices for testing cTnI, the scientific challenge that the low level of the marker in the blood of healthy patients means (at a molecular mass of cTnI of 24 kDa, 26 pg mL^{-1} correspond to 1.08 pM concentrations), and the commercial interest in sensitive, specific, robust, and affordable sensors spurred an unmatched race among biomolecular engineers for the development of new formats and examples of sensors that meet these requirements.

In this context, we intend to present in this short summary first a rather comprehensive (though probably not complete) list of examples in the literature of what other groups have reported. We will limit the compilation to the type of transduction principle that has been applied and the limit of detection (LoD) that has been achieved.

Then we use the results of our own studies to reflect on a few issues that one encounters in developing cTnI sensors. In particular, we will introduce 3 types of sensing concepts, based on:

- surface-plasmon optics (focusing on the most sensitive version offered by surface-plasmon fluorescence spectroscopy (SPFS)) [12],
- electrochemical assay, focusing on differential pulse voltammetry (DPV) [13],
- graphene FETs (gFET) as electronic sensors [14].

These sensors all measure in one way or another the surface coverage of the analyte molecules (cTnI in our case) that bind (reversibly) from solution to surface-immobilized receptors.

We present data for two types of receptors:

- antibodies [15],
- DNA aptamers [16].

Indeed, monoclonal antibody development involves several immunizations of a host animal, isolation of antibody-producing cells, followed by hybridoma selection and antibody production. Each step is time-intensive, with the entire process realistically taking four to six months. With aptamer selection being an *in vitro* process that is typically completed within 2-3 months, and together with increased shelf life of aptamers over antibodies with comparable affinity constants, these surface receptors lately are more intensively employed for sensing concepts [17].

In our examples, these receptors are immobilized using three types of chemistries typically applied by the community for the coupling of the receptor:

- Formation of self-assembled monolayers (SAMs) via thiol interaction with Au,
- π- π stacking interaction between 1-pyrenecarboxylic acid (PCA) and graphene followed by amide bond formation using EDC/NHS chemistry on the activated esters,
- Electroreduction of diazonium salts on graphene materials followed by Cu(I) based click-chemistry.

The substrates themselves represent three different types of substrate materials:

- Au for SPFS,
- Nitrogen-doped porous reduced graphene oxide (N-prGO) for the electrochemical studies,
- Graphene, prepared by chemical vapor deposition for the FETs.

And finally, we refer to two types of samples:

- cardiac Troponin I in PBS buffer, and
- clinical saliva samples.

We will discuss very briefly the essential basics of (and differences between) the various sensor platforms and compare the obtained results, in particular, with respect to the achieved LoDs in the light of the clinical requirements (cf. above).

2. Materials & Methods

2.1. Optical sensing

2.1.1. Surface-Plasmon Fluorescence Spectroscopy

For the direct optical analysis of the interaction between the protein and its receptors, antibodies in this case, an optical device combining surface plasmon resonance (SPR) [18] and surface plasmon-enhanced fluorescence spectroscopy (SPFS) [19, 20] in the Kretschmann configuration was used. The set-up consisted of a high refractive index (LaSF9) prism, optically matched to the sensor chip (50nm gold evaporated onto a LaSF9 glasss slide) and coupled to a flow cell. A laser beam at a wavelength of λ = 633 nm was directed to the prism base, and the reflected light collected by a photo detector in total internal reflection mode. The intensity was measured with a lock-in amplifier to observe changes in the SPR signal. At the appropriate angle of incidence, the enhanced electromagnetic field intensity generated by the resonant excitation of surface plasmons excites the chromophore-labelled analyte molecules bound from solution to the receptor units, immobilized on the sensor surface [21]. Their fluorescence signal was measured

(at λ = 670 nm) in this SPFS mode by a photomultiplier (H6240-01, Hamamatsu, Japan), linked to a photon counter. The beam intensity was reduced to 30-60 µW to avoid the bleaching of the employed chromophore Alexa Fluor 647. In order to separate the fluorescence light from scattered excitation light @ λ = 633 nm a set of filters (laser notch filter and fluorescence bandpass filter) was used.

2.1.2. Sensor Chip Preparation and Assay Development

LaSF9 high refractive index glass slides (Hellma Optics) were thermally evaporated-coated with 2 nm chromium and 50 nm gold, then incubated overnight in a 1:9 SH-PEG-COOH/ SH-PEG-OH (Sigma-Aldrich) solution for further surface functionalization. The SAM-coated gold slides were placed in the microfluidic flow cell with a volume of 4 µl. cTnI proteins were immobilized to the (EDC/NHS-) activated ester groups via amine coupling, and either monoclonal mouse or polyclonal goat antibodies (Abs) were rinsed across the cTnI capture layer. As a secondary antibody, AlexaFluor 647 conjugated anti-mouse or anti-goat antibodies were used at a concentration of 6 nM to monitor by SPFS the surface coverage of the primary ABs.

2.2. Electrochemical Sensing

2.2.1. Synthesis of N-prGO: The synthesis of prGO was achieved via dispersion of rGO powder (100 mg) in 30% H_2O_2 (100 mL), ultrasonicating for 30 min and heating for 12 h at 60 °C. The obtained solution was filtered and the recovered prGO powder was dialyzed to remove H_2O_2 and to separate from small sized graphene quantum dots [22].

The synthesis of N-prGO was carried out by mixing prGO powder and liquid ammonia (1:30 w/v) by ultrasonication before being transferred into a 50 mL Teflon coated stainless steel autoclave and heated for 24 h at 200 °C. The acquired solution was separated by filtration followed by washing with ethanol/water (1:1) mixture solution to completely remove the ammonia. The product was kept for drying in an oven at 60 °C overnight.

2.2.2. Preparation of the Electrodes: Glassy carbon electrodes (GC) were modified by drop-casting 5 µl of a suspension of N-prGO (1 mg ml^{-1} in water) and drying for 24 h in an oven at 60 °C. The formed GC/N-prGO electrodes were immersed in 0.1 M PBS (pH 7.0) and cycled 30 times between -1.5 V and +1.1 V at a scan rate of 0.1 V s^{-1} to stabilize the interface. Thereafter, to insure good reduction of the prGO, the potential was furthermore kept at -1.5 V for 3 min.

The GC/N-prGO electrode was immersed into a mixture of 1-pyrenecarboxylic acid (1 mM) and synthesised pyrene-PEG (1 mM) [23] with a ratio of 1:20 for 1 h at room temperature. The employed aptamer with the sequence 5'-NH_2-TTT TTT CGT GCA GTA CGC CAA CCT TTC TCA TGC GCT GCC CCT CTT A-3' was immobilized by first activating the carboxyl groups of 1-pyrenecarboxylic acid *via* immersion into a solution of EDC (15 mM)/ NHS (15 mM) in PBS (0.1 M, pH 7.4) for 30 min, followed by covalent coupling of the 5'-NH_2-modified aptamer (5 µL, 5 µM in PBS) by incubation for 40 min and washing (3 times) with PBS.

2.2.3. Differential Pulse Voltammetry: For the detection of cTnI, differential pulse voltammograms (DPV) [24] were recorded in a 5 mM $[Fe(CN)_6]^{4-}$ solution in 0.1 M PBS pH 7.4 within the potential range from -0.2 V to +0.5 V at a modulation amplitude of 5 mV and a step potential of 80 mV, step height of 15 mV and step time of 250 ms. Aptamer modified GC/N-prGO-COOH/PEG electrodes were immersed into cTnI standard solution or in samples containing cTnI for 30 min. After rinsing with PBS buffer (0.1 M, pH 7.4, three times), the electrodes were transferred into a 5 mM $[Fe(CN)_6]^{4-}$ solution in 0.1 M PBS pH 7.4 and a DPV signal was recorded. Following the measurements, immersion of the sensor into NaOH (0.1M, pH 12.0) for 20 min was used to regenerate the sensor interface.

2.3. Electronic Sensing Based on Graphene Field-Effect Transistors

2.3.1. Preparation of Functional Graphene Channels by "Click" Chemistry: For cTnI electronic sensing, we used a covalently-modified graphene field-effect transistor for the binding via "click" chemistry of a PEG-DNA aptamer mixture in a ratio of 1:2 [25]. Surface modification starts on a clean CVD-grown graphene after transferring it to an interdigitated electrodes device (Figure 1): first, electro-grafting of 4-((triisopropylsilyl)ethylenyl)benzenediazonium tetrafluoroborate (TIPS-Eth-ArN_2^+) (10 mM) in 0.1 M N-butylhexafluorophosphate (NBu_4PF_6) in acetonitrile was performed using cyclic voltammetry at a scan rate of 50 mV s^{-1} for five cycles between +0.30 V and -0.60 V vs. Ag/AgCl. The electrodes were rinsed with copious amounts of acetonitrile and acetone and gently dried. Before "click" chemistry, the TIPS protecting group was removed by the immersion of the Graphene-TIPS surface into tetrabutylammonium fluoride (TBAF, 0.1 M in THF) for 1h. The surface was then left for 15 min in a pure THF solution for cleaning. The deprotected surface was then exposed to a 1:2 mixture of methoxypolyethylene glycol azide (mPEG Azide, average MW 1000) and the DNA aptamer, using $CuSO_4$ (0.01 M) and L-ascorbic acid as reaction catalyst. The interface was treated with an aqueous solution of EDTA (10 mM) for 10 min to chelate any remaining Cu^{2+} residues and finally washed copiously with water and left to dry.

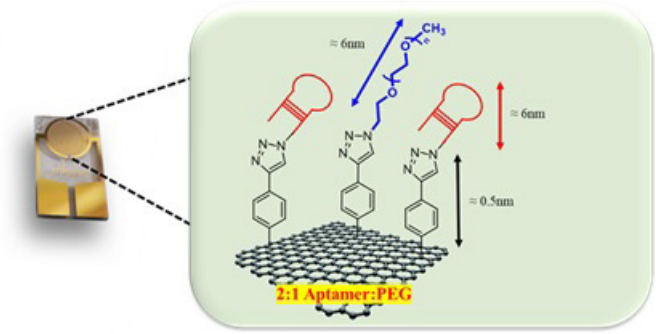

Figure 1: Graphene based field effect transistor surface-modified by anti-fouling PEG chains and aptamers for specific cTnI sensing

2.3.2. Electronic Read-out of cTnI Binding: Graphene transfer characteristics were recorded after each modification step using a Keithley 2400 source-meter with custom-made LabVIEW software. All measurements were performed using a MicruX flow cell made of PMMA with fixed flow channel geometry (16 µl), ensuring a defined flow rate of 50 µl min^{-1} to minimize mass transport limitation of the analyte to the sensor surface in all experiments [26]. Electrical measurements were performed by applying a 50 mV source−drain bias V_{DS} and sweeping the gate potential V_{GS} while monitoring the current between the drain and the source I_{DS}. A silver chloride wire (diameter 1 mm, Sigma-Aldrich) was used to operate the graphene-FET device in liquid gate configuration, with a constant gate bias of 0.2 V. The general procedure of the sensing experiment started with continuously flushing the pure buffer (PBS, 0.01x) until a stable baseline of drain current was established, followed by injection of the analyte at a constant flow rate [27].

3. Results

The long list of papers published on the detection of cTnI is given in Table 1, containing a total of 120 references, with the first paper published in 2004.

The spectrum of the applied detection principles is rather wide, with a clear focus on optical (including surface-plasmon resonance (SPR), fluorescence, colorimetric, fluorescence resonance energy transfer (FRET)), as well as electrochemical techniques (e.g., cyclic- or differential pulse- voltammetry, impedimetric protocols, electro-chemiluminescence, etc.). However, also a few exotic detection formats for the monitoring of cTnI as a marker for AMI events have been reported; e.g., surface-enhanced resonance Raman spectroscopy (SERRS), magneto-optics, single-photon detection, electro-acoustic principles, to mention but a few. In addition, several reports appear in the literature on the use of electrical or electronic concepts for cardiac marker sensing.

Concerning the transducer functionalization as a means to guarantee the mere specific recognition and binding of the analyte proteins, three receptor systems have been described; i.e., antibodies, peptides, and aptamers.

Most remarkable in this long list of references is the incredible spread of reported limits of detection (LoD), ranging from $7.7x10^{5}$ pg mL^{-1} to $4.8x10^{-4}$ pg mL^{-1}, thus covering 9 orders of magnitude!

Given the current cut-off level for cTnI in healthy patients of 26 pg mL^{-1}, one half of the reported tests have only historical value and don't need to be considered further: no clinic would use any of these principles and protocols.

At the other end of the spectrum, extreme sensitivities seem to be offered with spectacular LoDs – but not for free: in all cases, the reported values are the result of extreme complexities with multiple amplification steps – totally useless for practical applications: doctors need simple and easy to apply tests and recipes. And not even from a scientific point of view any of these reports on "ultra-sensitive" sensors is helpful: none of the authors dares about trying to understand the basic physical principles that might operate in their experiment! The simple question: what is the molecular mechanism and/or a theoretical model by which one could understand that the sensor response changes by a factor of 3-5 (!) upon varying the cTnI concentration by 5-7 orders of magnitude [28-32] (Calling this "linear" is another story…). All reports refer to a bimolecular reaction between the ligand, cTnI, and its antibody or specific aptamer. A description of this reaction by a Langmuir model might be too simple; however, it would be a good starting point: it would explain that there might be a truly linear regime at concentrations well below the half-saturation concentration, i.e., the dissociation constant, K_d, for the specific receptor-ligand pair! And it would suggest that there should be a saturation behavior for analyte concentrations in the sample solution well-above this K_d-value.

In order to explain why it is so important to generate this model-based understanding of the molecular interactions on the sensor surface, we refer to our own work and summarize in the following experimental binding data that were collected by i) surface plasmon fluorescence spectroscopy, by ii) an electrochemical technique, i.e., differential pulse voltammetry, and by the most recent methodological developed in our laboratories, i.e., iii) an electronic read-out concept based on graphene field-effect transistors (gFETs).

3.1 Optical cTnI Sensing Based on Surface-Plasmon Fluorescence Spectroscopy

Because a direct detection format with mere SPR readout provided insufficient sensitivity, the first example that we present is an approach based on surface-plasmon fluorescence spectroscopy with a special inhibition immune assay [33]. As shown in Figure 2, this assay consisted of three steps: firstly, samples with known concentrations of cTnI were spiked in the bulk solution with mouse monoclonal anti-cTnI antibodies, each at a concentration of 2 nM, and incubated for 20 min (Figure 2(a)). Theses samples were then flowed for 20 min over the surface of a sensor chip that was prepared with cTnI proteins immobilized onto a mixed thiol SAM with active ester groups coupled to the amine moieties of the proteins (Figure 2(b)). And finally, after rinsing for 5 min, a 6 nM solution of a secondary Alexa Fluor 647-conjugated anti-mouse antibody was allowed to react with the affinity bound primary antibody (Figure 2(c)). After another 5 min of rinsing, the fluorescence sensor response ΔF was determined. Due to the competitive binding in the reaction vessel, the sensor response shows an increase with decreasing analyte concentration, as seen in Figure 2(d). In a solution with low concentration of cTnI analyte, most binding sites of the a-TNNI3 antibody are available and attach to the sensor surface with the immobilized cTnI. This way, a high fluorescence signal is seen after the reaction with the labelled secondary antibody. At a high concentration of the cTnI target analyte present in the bulk solution, the binding sites of the a-TNNI3 antibody are occupied, thus leading to low fluorescence signal on the sensor chip.

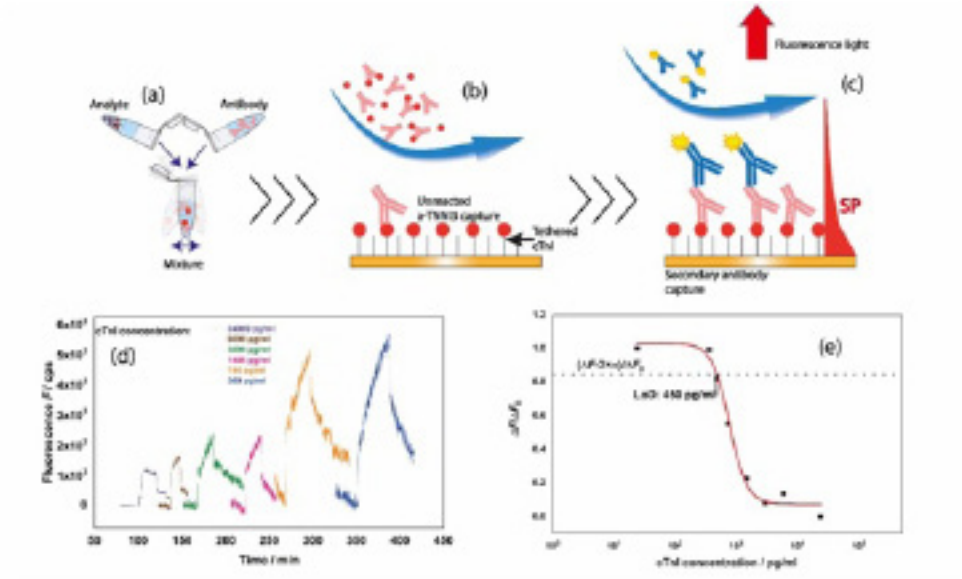

Figure 2: Schematics of the competitive assay, consisting of (a) mixing of the analyte (of known concentrations for the calibration curve) with a known concentration of a primary antibody; (b) flowing the mixture across the chip surface of the sensor which was functionalized by a monolayer of immobilized cTnI; (c) rinsing the flow-cell with the fluorescently labelled secondary antibodies, and (d) recording the fluorescence signal of the binding of the secondary antibody. (e) fluorescence signal, taken from (d) as a function of the cTnI concentration in the bulk mixture.

The 3 σ-limit of detection (LoD) derived from the response of the fluorescence signals plotted as a function of the cTnI concentrations (Figure 2(e)) was 450 pg mL^{-1}, below the most recently clinically defined threshold for diagnostically relevant levels of cardiac troponins.

3.2. Electrochemical Determination of cTnI Levels by Differential Pulse Voltammetry

Carbon-based materials [34] are promising candidates for the sensitive detection of medically relevant markers like cTnI by electrochemical means [35]. We added lately to this field by proposing the use of nitrogen-doped porous reduced graphene oxide (N-prGO) [36] for detection and quantification of cTnI (Figure 3a). The good electrochemical conductivity (Figure 3b) of N-prGO, formed by a two-step process from reduced graphene oxide by first treatment with hydrogen peroxide (H_2O_2) and subsequent hydrolysis of the formed epoxy groups to hydroxyl groups, accompanied by C-C bond breaking to produce a rGO porous structure, is one important element in this sensor. Coupling of an aptamer, known for its high selectivity towards cTnI [37], via 1-pyrenecarboxylic acid and the presence of an antifouling element such as PEG-based pyrene ligand, are other important elements in this approach.

Addition of cTnI of different concentrations to these interfaces results in a decrease of the maximum current as recorded by differential pulse voltammetry with $[Fe(CN)_6]^{4-}$ as redox probe (Figure 4a). This change is proportional to the cTnI concentration between 1 pg mL^{-1} and 100 ng mL^{-1} with a detection limit of about 0.88 pg mL^{-1} (Figure 4b).

Interestingly, this sensor concept allows also for sensing of cTnI in

saliva samples of patients who reported chest pain. The sensitivity of the sensor changes when working in saliva due to the presence of a large variety of proteins and salts (Figure 4c), but a comparable LoD of 1 pg mL^{-1} could still be reached. The electrochemical response of a saliva sample of a healthy and an AMI diagnosed patient could be differentiated (Figure 4d). cTnI concentrations of below 1 pg mL^{-1} were determined for the healthy patients, while a cTnI level of 675 pg mL^{-1} was determined for the AMI diagnosed patients. In the case of the healthy patients, the quantitation limit of the sensor was just good enough to indicate that the concentration is below 1 pg mL^{-1}.

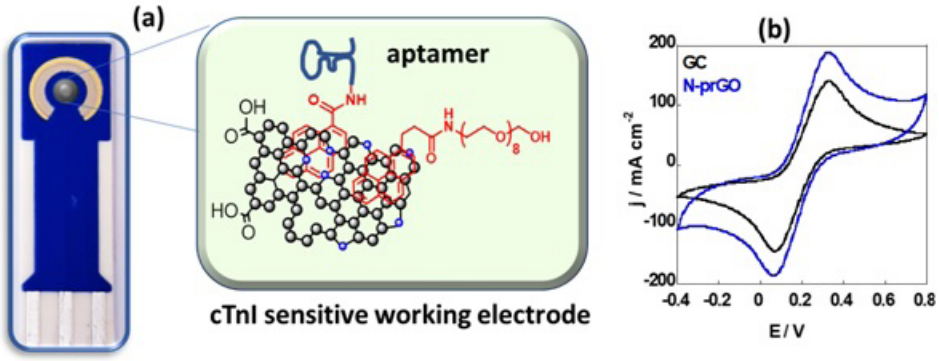

Figure 3: (a) Concept of the electrochemical cTnI sensor based on drop casting N-prGO onto the carbon working electrode followed by modification with 1-pyrenecarboxylic acid and poly (ethylene glycol) (PEG) modified pyrene ligand and covalent integration of an aptamer onto the1-pyrenecarboxylic acid functions. (b) Cyclic voltammograms recorded on GC (black), and GC coated with N-prGO (blue) using $[Fe(CN)_6]^{4-}$ (5 mM)/PBS (0.1M)) as redox mediator, scan rate = 100 mV s^{-1}.

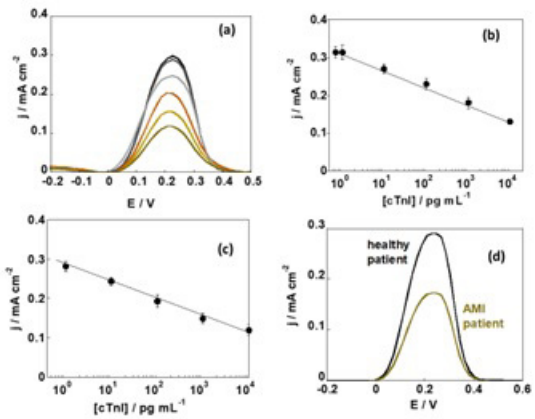

Figure 4: (a) Differential pulse voltammograms at various cTnI concentrations (0, 0.001, 0.01, 0.1, 1 and 10 ng mL^{-1}) in PBS ×1 (pH 7.4). (b) Calibration curve in PBS ×1 (pH 7.4). (c) Calibration curve for cTnI in human saliva samples spiked with different concentrations of cTnI. (d) DPV curves in saliva of patient samples with chest pain and diagnosed AMI and healthy ones as controls.

3.3. Electronic Sensing Based on Graphene Field-Effect Transistors

FET-based biosensors, properly functionalized by a selective receptor layer, will directly convert any biological interaction into an electrical signal [38], allowing also for real-time detection of cTnI with high sensitivity and selectivity. This measured current signal is due to the accumulation of charge carriers in the channel caused by a modulation of the gate potential, which in turn is influenced by the presence of the analyte bound to its receptor. In particular, graphene as a channel material in FETs has many interesting properties that make it attractive for biosensing including, high sensitivity to near surface charges and electric fields, excellent electrical characteristics (high mobility, high transfer kinetics, high conductivity, among others), as well as good mechanical properties and biocompatibility [39, 40].

After coupling the 2:1 aptamer: PEG layer by “click” chemistry to the graphene channel of the transistor (cf. section 2.c1), the transfer characteristics of the modified-graphene FET during exposure to cTnI solutions with concentrations ranging from 3 to 1000 pg mL^{-1} were recorded after stabilization with each concentration (Figure 5a). At different cTnI concentrations, an increase of the FET source-drain current is observed in the holes’ regime and a decrease in the electrons’ regime. This comes as a consequence of the positively charged molecules adsorbed onto the channel – since

cTnI has the isoelectric point at pH 9.87, it is positive in PBS at pH 7.4. This will induce a negative charge in the graphene channel, generating more electrons, leading them to become the majority carriers; the I_DV_G curve shifts to the left side due to graphene's n-doping, leading to a decrease of the central neutrality point (CNP) also known as Dirac point. This suggests that the decrease of the Dirac point value is attributed to the charge gating effect of the attached linker molecules and cTnI. The sensor response was analyzed at a gate voltage of 350 mV – at this value, the current for each cTnI concentration and for the PBS 0.01x baseline was extracted from the I_DV_G curve. By calculating $\Delta I_{DS} = I_{DS}$ ([cTnI]$_n$) – I_{DS} ($PBS_{0.01x}$), for each given concentration, n, in pg mL^{-1}, a calibration curve was obtained (Figure 5b). The fit of these data to a Langmuir model (black curve in (Figure 5(b)) gave a dissociation constant of K_d = 55 pg mL^{-1}. As judged from the minimal difference of the source-drain-current at V_G = 350 mV (cf. Figure 5a) between pure buffer and the 3 pg mL^{-1} solution we estimate a LoD = 1 pg mL^{-1}.

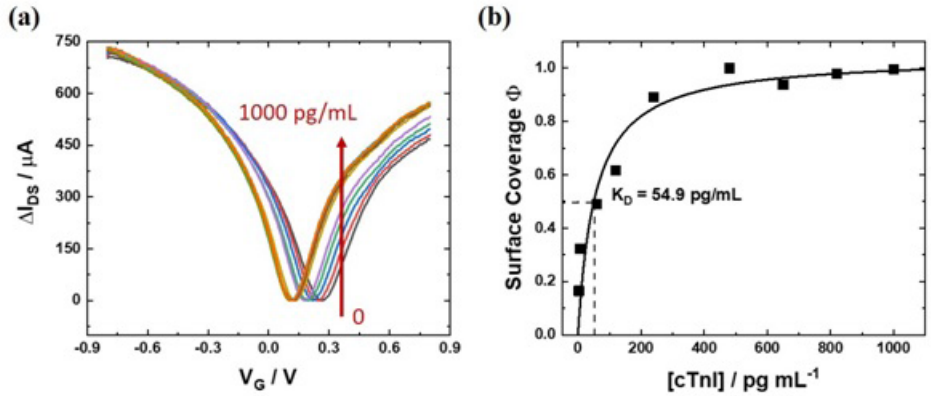

Figure 5: (a) Graphene transfer characteristics (ΔI_{DS}-*vs*-V_G curves) after stabilization with each cTnI concentration (0, 3, 6, 60, 120, 240, 480, 650, 820 and 1000 pg mL^{-1}) in 0.01x PBS (pH 7.4) without washing steps. (b) ΔI_{DS}, converted according to the Langmuir model to the corresponding surface coverage, Φ, as a function of the analyte concentration of the solution running through the flow cell.

4. Discussion

We start the discussion with a few fundamental remarks concerning the use of biosensors as analytical tools for monitoring the concentration of clinically relevant markers in body liquids like whole blood, plasma, urine, saliva, or others. For any one of the concepts developed for monitoring the cardiac marker cTnI that were reported in the literature (cf. Table 1) the optical, electrochemical or electronic transducers were all functionalized, each with a layer of specific receptor molecules. For cTnI, these receptors were either specific antibodies, peptides (derived from phage-display approaches), or aptamers. These functional coatings are optimized to serve a double purpose for the transducer that will be exposed to the analyte solution: on the one side, it offers specific sites with a typically high binding affinity for the analyte molecule of interest; and on the other side, it passivates the sensor surface by an anti-fouling coating which prevents all other molecules in the cocktail of the analyte solution from binding as well, thus preventing a possibly strong background sensor signal from non-specific binding events.

Upon exposure of such a functionalized transducer surface to the analyte solution (some of) the empty binding sites will be occupied by the association (binding) of the analyte molecules from the bulk. If the binding is reversible, i.e., if the analyte can also dissociate again, the surface coverage, i.e., the fraction of occupied binding sites of the receptor (mono-)layer establishes an equilibrium with the corresponding bulk concentration – which is the level of the marker of interest in the test sample. This one-to-one correlation between the bulk concentration of the marker and its surface density on the sensor surface is the basis for the quantitative evaluation of the marker concentration in the test solution from a measurement of its surface coverage on the transducer device used.

The sensitivity of any sensor depends critically on two factors: the first is the binding affinity of the analyte molecule to the receptor molecule. This receptor affinity can be quantified by an inhibition constant or K_d value, which indicates the bulk concentration required to occupy 50% of the receptor molecules on the transducer surface; hence, it is also called half-saturation constant. Obviously, the lower this constant, the lower the bulk concentration can be to reach half-saturation on the sensor. This is the motivation for the race towards high-affinity receptors, e.g., by the SELEX process for the development of high-affinity aptamers [41], or the search for high affinity antibodies [42].

The second factor that is crucial is a feature of the transducer itself and depends on its principle of operation: it reduces to the simple question: how low in coverage, well below half-saturation, can one still see a sensor signal upon the binding of only a few ligands to the receptor molecules. Given the broad diversity of transducer principles developed for biosensors, there

is no general answer to this question and depends heavily on the physics behind the transduction concept implemented. The only common feature frequently observed is the use of labels that are introduced with the sole purpose, i.e., to enhance the signal contribution of each analyte molecule to the overall sensor response. The well-established enzyme-linked immunosorbent assay (ELISA) is a classic example for that concept and was developed to enhance via enzymatic amplification the signal from each binding event.

For the examples for cTnI detection from our own group presented above, the fluorescence-labeling of the antibodies used in our surface-plasmon optical detection approach falls into this category: the binding of an antibody to the ligand cTnI is further enhanced by recording the fluorescence emission originating from a secondary chromophore-labeled (detection) antibody binding to the first one. The multiple cycling between the ground and the excited state of the chromophore with the emission of up to 2000 photons per second per dye molecule [43] represents an enhancement factor of the detection scheme that increases the sensitivity significantly. It should be pointed out that it is not the analyte that needs to be labelled, but the secondary antibody. Hence, this is not a serious limitation of this and similar techniques; however, it means an additional processing step. Similarly, the example given for the category of electrochemical sensors based on the modification of the differential pulse voltammetric signal upon the binding of cTnI to an aptamer binding layer depends on the surface coverage and thus generates a sensor signal that is strictly correlated with the binding events of interest. In this example, the mechanism for enhancement is the redox cycling of the mediator $[Fe(CN)_6]^{4-}$. Only the electronic sensing platform discussed as the third example monitors the binding of cTnI from a solution sample to the aptamer receptor layer by the direct impact of analyte molecules (and possibly the resulting impact on the receptor, e.g., a change in the charge distribution by a reorganization in the structure of the aptamer) on the source-drain current of a field-effect transistor tuned to an appropriate gate voltage (V_G = 350 mV in this case).

With this in mind, we are now turning to the surface-plasmon optical sensor data. The concept that we focus on is based on a particular format, an inhibition immuno-assay: the first step is the mixing of the sample solution of the appropriate antibody, the receptor R, of known concentration, c_R, with the marker molecules, the ligands L, at concentration, c_L. According to the reaction ([44], cf. also Figure 2(a)):

the concentration of the ligand-receptor complex, c_{RL}, is determined by the equilibrium constant, K_A, (the inverse of the dissociation constant (half-saturation constant), $K_d = k_d / k_a$,) given by the mass action law

$$K_A = c_{RL} / c_R \cdot c_L. \qquad \text{Eqn. (1)}$$

The unreacted, still empty receptor molecules together with the formed complexes are then rinsed through the flow cell across the transducer surface of the SPFS spectrometer (Figure 2(b)), bind to the surface-immobilized cTnI ligands, and are detected via a secondary chromophore- labeled antibody (Figure 2(c)), the fluorescence of which is monitored. For very low concentrations of the ligand in the reaction vessel, only a small fraction of the receptor molecules is occupied; hence, leads to a high fluorescence signal (cf. Figure 2(d)). Increasing successively the ligand concentration in the reaction vessel, occupies more and more of the receptors; hence, the fluorescence signal decreases (Figure 2(d)). The result is a titration curve of the receptor in the bulk solution of the reaction vessel (Figure 2(e)), the fit of which according to eqn. (1) yields the dissociation constant K_d = 840 pg mL^{-1} (corresponding to K_d = 35 pM). The 3σ- criterion for the limit of detection leads to LoD = 450 pg mL^{-1}. For the first generation of troponin assays in the clinic, this result was good enough; however, despite representing a very attractive high affinity constant for an antigen-antibody interaction, the progress in high-sensitivity troponin tests with their progressively lowered cut-off level for healthy patients nowadays asks for better performance assays. It should be pointed out, although, that it was not so much the affinity of the employed antibody that limits the applicability of the assay, it was the moderate LoD, compared to the K_d-value of the interaction that acts as the show stopper: because of the inversion of the signal generation – a low level of ligands in the bulk solution means a high fluorescence signal on the sensor and vice-versa - a relatively high background fluorescence at low analyte concentrations leads to a difference between K_d and LoD of only a factor of 2, very different from the best cases of an SPFS-based biosensor assay reported in the literature [45] where for the detection of a (fluorescently labelled) 196bp PCR amplicon by a PNA capture probe on the sensor surface, a LoD = 100 fM was achieved at a K_d value of 2.7 nM, i.e., a ratio of LoD / K_d = 1 / 30000!

The next example that we presented was based on differential pulse voltammetry with $[Fe(CN)_6]^{4-}$ as the redox mediator, and using a specific aptamer, taken from the literature [37] as the receptor system for cTnI binding to this sensor surface from the analyte solution. A key concept in electrochemical systems is the fact that the kinetics of the heterogeneous electron transfer is modulated upon ligand-analyte interactions. Using the negatively charged ferrocyanide redox couple $[Fe(CN)_6]^{4-}$ revealed that electron transfer is increasingly hindered upon interaction of the positively charged cTnI analyte (theoretical isoelectric point 9.87) with the surface linked aptamer most likely due to restricting the diffusion. With a LoD of 0.88 pg mL^{-1} in PBS and 1 pg mL^{-1} in saliva, this concept is a very attractive alternative to other techniques described in the literature. The simplicity of the method and the portable character of the sensor format makes, this approach appealing as point-of-care testing (POCT) device.

Table 1: Compilation of publications reporting on the detection of cTnI. Given are the LoD (all values scaled in units of pg mL^{-1}, with 24 pg mL^{-1} = 1 pM) and year of publication, together with the analytical technique applied: SPR, surface-plasmon resonance; CL, chemiluminescence; FRET, fluorescence recovery after photobleaching; SPFS, surface-plasmon fluorescence spectroscopy; ECL, electro-chemiluminescence; FET, field-effect transistor; SE(R)RS, surface-enhanced (resonance) Raman spectroscopy; SAW, surface acoustic wave.

Applied Technique		LoD pg ml^{-1}	Year	Ref.
Fluorescence	QD	770000	2008	[46]
Electrochemical	Peptides	340000	2010	[47]
Electrochemical		16000	2017	[48]
SPR	Au nanorod	10000	2009	[49]
SPR		6800	2011	[50]
CL	ELISA	5600	2007	[51]
Fluorescence	Aptamers	5000	2015	[52]
SPR		5000	2016	[53]
SPR		1400	2004	[54]
SPR		1250	2017	[55]
Electrochemical	Aptamers	1190	2014	[56]
Electrochemical	AuNPs	1000	2011	[57]
Electrochemical	Conducting paper	1000	2012	[58]
Chemiresistor	ZnO NP	1000	2016	[59]
Electrochemical	Antibody	800	2021	[60]
FRET		700	2009	[61]
Electrochemical	MIP	650	2016	[62]
Paramagnetic	Magnetic NPs	500	2007	[63]
SPFS	Antibody	450	2020	[64]
Electrochemical	AuNPs	250	2013	[65]
Impedimetric		200	2010	[66]
Electrochemical	AuNPs	200	2012	[67]
Colorimetric	Peptides/AuNP	200	2016	[68]
Electrochemical microchip		148	2007	[69]
ECL		110	2018	[70]
Fluorescence	Fluoro-microbead	100	2011	[71]
Electrochemical	Au and Ag	100	2013	[72]
Fluorescence	AMPPD-ALP	100	2014	[73]
Photonic Xtal	Antibodies	100	2014	[74]
FRET	Antibody	97	2020	75]
FET	Silicon nanowire	92	2012	[76]
Paramagnetic	Magnetic NPs	72	2009	[77]
Electrochemical		70	2016	[78]
Fluorescence	Aptamer	70	2018	[79]
SPR	Peptides	68	2011	[80]
ECL	AuNPs	60	2013	[81]
Electrochemical	Nanocomposites of AuNPs	50	2016	[82]
Electrochemical	Antibody	50	2020	[83]
Cyclic voltammetry		40	2018	[84]
Paramagnetic	Magnetic NPs	30	2010	[85]
Colorimetric	HRP	27	2009	[86]
Electrochemical		25	2015	[87]
Electrochemical	Antibody/Aptamer	24	2015	[37]
Electrochemical	Aptamer	24	2017	[88]
Electrochemical	DNA	24	2019	[89]
Electrochemical	Aptamer	23	2018	[90]
Fluorescence		16	2018	[91]
Electrochemical	Aptamer 1	16	2019	[92]
SERRS	AuNP	16	2020	[93]
SPR/electric	Antibody	15	2018	[94]
Electro-acoustic	Antibody	14	2020	[95]
Optomagnetic		11.7	2009	[96]
ELISA		10	2009	[97]
Colorimetric	AuNP	10	2010	[98]

Colorimetric	AuNPs	10	2010	[99]
Chemiresistor	SWCNT/ AuNP	10	2013	[100]
Potentiometric		10	2014	[101]
Electrochemical		10	2018	[102]
Electrochemical	Array of Au NPS Aptamers	8	2017	[103]
CMOS Transistor	Antibody	7.7	2014	[104]
Chemiresistor	Nanowire, Antibody	7.7	2015	[105]
Electrochemical	Aptamer	7.5	2019	[106]
SAW	AuNPs	6.2	2013	[107]
AlGaN/GaN transistor		6	2018	[108]
Electrochemical		6	2018	[109]
Electrochemical	Aptamer	5.7	2019	[110]
Optical	Antibody	5.7	2020	[111]
Fluorescence	Antibody	5.6	2020	[112]
Fluorescence	FITC	5	2011	[113]
SERS	Graphene-Au NP	5	2019	[114]
Electrical	Silicon nanowire	5	2016	[115]
Electrochemical	Aptamer	4.3	2019	[116]
Electrochemical	Pt nanoparticles	4.2	2014	[117]
Electrochemical	QD	4	2010	[118]
Electrochemical	Au NPs	3.4	2016	[119]
FET	ZnO NPs	3.24	2017	[120]
Electrochemical		2.4	2016	[121]
ELISA		2	2010	[122]
ECL	AuNPs	2	2011	[123]
Fluorescence	Europium(III)	2	2012	[124]
Chemiresistor	Antibody	1	2014	[125]
Chemiresistor	Antibody	1	2014	[126]
Impedimetric		1	2016	[127]
Impedimetric		1	2017	[128]
Electrochemical	Aptamer	1	2018	[129]
Electrochemical	Aptamer	1	2018	[36]
Electrochemical	Graphene-multi walled carbon	0.94	2015	[130]
CL	Antibody	0.84	2020	[131]
ECL	Au NPs	0.5	2015	[132]
ECL	Aptamer	0.48	2019	[133]
Electrochemical	Au NPs Ru-peptide	0.4	2014	[134]
Chemiresistor	Nanowire, Antibody	0.25	2012	[135]
Paramagnetic	Antibody	0.2	2007	[136]
Electrochemical		0.17	2018	[137]
SPR	Antibody	0.12	2020	[138]
Fluorescence	TiO2 nanotube array AM700	0.1	2012	[139]
Electrochemical	Aptamer	0.05	2020	[140]
Electrochemical		0.033	2019	[141]
ECL		0.016	2015	[142]
ECL	AuNPs	0.012	2017	[143]
Electrochemical		0.01	2011	[144]
Photoelectrochemical		0.0067	2018	[28]
ECL	Antibody	0.004	2019	[29]
Electrical	Aptamer	0.0024	2020	[30]
Fluorescence	Antibody	0.00084	2013	[31]
ECL	Antibody	0.00048	2019	[32]

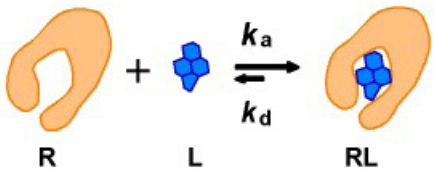

The last example from the set of techniques that we applied for the development of a sensitive cTnI test assay was based on a transistor device using graphene as the channel material that connects source and drain electrodes. The functionalization of this channel by a diazonium-based coupling strategy with the attachment of the cTnI-specific aptamer [37] by click chemistry leads to a very promising I_DV_G behavior (cf. Figure 5(a)), indicating excellent mobilities in the device structure. Even more important is the very reproducible (and reversible [44]) shift of the individual I_DV_G-curves upon rinsing analyte solution through the flow cell. The observed behavior is given only by a shift of the Dirac point to lower positive voltages, in line with the understanding that the binding of the analyte protein leads to an aptamer/cTnI complex at the sensor surface that results in a gradual change of the surface potential at the channel/analyte solution interface that adds to the gate voltage.

By plotting the change of the source-drain current, I_{DS}, taken at a constant gate voltage of V_G = 350 mV as a function of the cTnI concentration, we observed a behavior that suggested an analysis in terms of a classic binding behavior: for low concentrations, the current increased linearly with the cTnI concentration, to then merge into a saturation behavior at higher concentrations (Figure 5(b)). Assuming a Langmuir binding model these data can be fitted with the dissociation constant as the only parameter, resulting in K_d = 55 pg mL^{-1} (corresponding to about 2.5 pM). This is a remarkably high affinity for an aptamer as receptor for a bio-affinity reaction and a good starting point for a very sensitive assay for clinical applications. The obtainable LoD is certainly better than 1 pg mL^{-1}, as judged from the clear difference of the I_DV_G-curves measured in bare PBS-buffer and after injecting a cTnI-solution with a concentration of only 3 pg mL^{-1}. With these limits, the approach falls definitely into the regime of assays with a clinically relevant resolution: the cut-off level of assays of even the third generation is defined as 26 pg mL^{-1} for healthy individuals.

5. Conclusion

In recent years, the cardiac marker, cTnI, obviously became a reference system heavily used by the community of biosensor developers to calibrate their broad range of transducer concepts and experimental setups. The result is a long list of publications dealing with just this one marker, quantifying its LoD as the clinically relevant parameter. As mentioned before, the range of LoD values reported in the literature is covering 9 orders of magnitude! However, a relatively large number of papers is only (at best) of historical value because todays cut-off requirements for clinical applications are at the level of 26 pg mL^{-1} (to be able to monitor also healthy patients), although one has to admit that the cut-off level was constantly decreasing over the years: what used to be a good technique for the detection of the cTnI level in patients' blood a few years ago is not acceptable any more today. Still, the list of reports with LoDs in line with the current clinical levels is impressive. Hence, a practitioner looking for a good detection concept for cTnI needs to take into consideration other factors of the test kit like the ease of operation, the robustness of the test kit, the costs, etc. Hence, it can be expected that even in the foreseeable future there will be new proposals for and reports about better devices that may eventually also be marketable and will find their way into the clinic of doctor's office. We, too, continue to work on that target.

6. Acknowledgement

Financial support from the Centre National de la Recherche Scientifique (CNRS), the University of Lille, the Hauts-de-France region, and the CPER "Photonics for Society", are acknowleged.

References

1. https://www.who.int/health-topics/cardiovascular-diseases#tab=tab_1
2. http://www.championadvocates.org/en/champion-advocates-programme/the-costs-of-cvd
3. McDonnell B, Hearty S, Leonard P, Richard O'Kennedy R. Cardiac biomarkers and the case for point-of-care testing. Clinical Biochem. 2009; 42(7–8): 549-61.
4. Han X, Li S, Peng Z, Othman AM, Leblanc R. Recent Development of Cardiac Troponin I Detection. ACS Sens. 2016; 1(2): 106–11
5. Szunerits S, Mishyn V, Grabowska I, Boukherroub R. Electrochemical cardiovascular platforms: Current state of the art and beyond. Biosens Bioelectron. 2019; 131: 287-98.
6. Hamm CW, Goldmann B, Heeschen C, Kreymann G, Berger J, Meinertz T. Emergency Room Triage of Patients with Acute Chest Pain by Means of Rapid Testing for Cardiac Troponin T or I. N. Engl. J. Med. 1997; 337: 1648-53.
7. Upasham S, Tanak A, Prasad S. Cardiac troponin biosensors: where are we now? Advanced Health Care Technologies. 2018; 4: 1-13.
8. https://www.mlo-online.com/continuing-education/article/21121636/implementation-of-highsensitivity-cardiac-troponin-into-clinical-practice.
9. Romiti GF, Cangemi R, Toriello F, Ruscio E, Sciomer S, Moscucci F, et al. Sex-Specific Cut-Offs for High-Sensitivity Cardiac Troponin: Is Less More? Cardiovasc Ther. 2019; 9546931.
10. Kontos MC, Anderson FP, Alimanrd R, Ornato JP, Tatum JL, Jesse RL. Ability of troponin I to predict cardiac events in patients admitted from the emergency department. J Am Coll Cardiol. 2000; 36(2000) 1818-23.
11. Maqsood A, Kaid K, Cohen M. Clinical Significance of Borderline Cardiac Troponin (cTnI) in Patients Presenting with Acute Coronary Syndrome who are Referred for Cardiac Catheterization. The Internet Journal of Cardiovascular Research. 2006; 4: 1-4.
12. Sergelen K, Fossati S, Turupcu A, Oostenbrink C, Liedberg B, Knoll W, et al. Plasmon field-enhanced fluorescence energy transfer for hairpin aptamer assay readout, ACS sensors. 2017; 2(7): 916-23.
13. Vasilescu A, Wang Q, Li M, Boukherroub R, Szunerits S. Aptamer-

Based Electrochemical Sensing of Lysozyme. Chemosensors. 2016; 4(2): 10.

14. Syu YC, Hsu WE, Lin CT. Review—Field-Effect Transistor Biosensing: Devices and Clinical Applications. ECS Journal of Solid State Science and Technology. 2018; 7(7): Q3196-207.
15. Saeed AFUH, Wang R, Ling S, Wang S. Antibody Engineering for Pursuing a Healthier Future. Front. Microbiol. 2017; 8: 495.
16. Zhang Y, Lai BS, Juhas M. Recent Advances in Aptamer Discovery and Applications, Molecules. 2019; 24(5): 941.
17. Bognár Z, Gyurcsányi RE. Aptamers against Immunoglobulins: Design,Selection and Bioanalytical Applications. Int. J. Mol. Sci. 2020; 21: 5748.
18. Knoll W. Interfaces and Thin Films as Seen by Bound Electromagnetic Waves. Ann. Rev. Phys. Chem. 1998; 49: 569-638.
19. Knoll W, Kasry A, Liu J, Neumann T, Niu L, Park H, et al. Surface Plasmon Fluorescence Techniques for Bio-Affinity Studies Handbook of Surface Plasmon Resonance, Eds. R.B.M. Schasfoort and Anna J. Tudos Chpt. 2008; 9: 275-312.
20. Liebermann T, Knoll W. Surface-plasmon field-enhanced fluorescence spectroscopy. Colloids and Surfaces A: Physicochemical and Engineering Aspects. 2000; 171(1-39): 115-30.
21. Yu F, Persson B, Lofas S, Knoll W. Atto-Molar Sensitivity of Surface Plasmon Fluorescence Spectroscopy, J. Am. Chem. Soc. 2004; 126: 8902-3.
22. Singh SK, Dhavale VM, Boukherroub R, Kurungot S, Szunerits S. N-doped porous reduced graphene oxide as an efficient electrode material for high performance flexible solid-state supercapacitor Appl Mater. Today. 2017; 8: 141-9.
23. Barras A, Szunerits S, Marcon L, Monfilliette-Dupont N, Boukherroub R. Functionalization of Diamond Nanoparticles Using "Click" Chemistry, Langmuir. 2010; 26: 13168-72.
24. Selvam SP, Chinnadayyala SR, Cho S, Yun K. Differential Pulse Voltammetric Electrochemical Sensor for the Detection of Etidronic Acid in Pharmaceutical Samples by Using rGO-Ag@SiO2/Au PCB. Nanomaterials. 2020; 10(7): 1368.
25. Mishyn V, Aspermair P, Leroux Y, Happy H, Knoll W, Boukherroub R, Szunerits S. "Click" Chemistry on Gold Electrodes Modified with Reduced Graphene Oxide by Electrophoretic Deposition. Surfaces. 2019; 2: 193-204.
26. Aspermair P, Mishyn V, Bintinger J, Happy H, Bagga K, Subramanian P, et al. Reduced graphene oxide–based field effect transistors for the detection of E7 protein of human papillomavirus in saliva. Anal. Bioanal. Chem. 2021; 413(3): 779-87.
27. Reiner-Rozman C, Larisika M, Nowak C, Knoll W. Graphene-based liquid-gated field effect transistor for biosensing: Theory and experiments. Biosens. Bioelectron. 2015; 70: 21-7.
28. Chen J, Kong L, Sun X, Feng J, Chen Z, Fan D, Wei Q. Ultrasensitive photoelectrochemical immunosensor of cardiac troponin I detection based on dual inhibition effect of Ag@Cu2O coreshell submicron-particles on CdS QDs sensitized TiO2 nanosheets. Biosens Bioelectron 2018; 117: 340-6.
29. Ye J, Zhu L, Yan M, Zhu Q, Lu Q, Huang J, et al. Dual-Wavelength Ratiometric Electrochemiluminescence Immunosensor for Cardiac Troponin I Detection. Analytical Chemistry. 2019; 91(2): 1524-31.
30. Zhang J, Lakshmipriya T, Gopinath SCB. Electroanalysis on an Interdigitated Electrode for High-Affinity Cardiac Troponin I Biomarker Detection by Aptamer–Gold Conjugates. ACS Omega. 2020; 5(40): 25899-905.
31. Lee S, Kang SH. Quenching Effect on Gold Nano-patterned Cardiac Troponin I Chip by Total Internal Reflection Fluorescence Microscopy. Talanta. 2013; 104: 32-8.
32. Yan M, Ye J, Zhu Q, Zhu L, Huang J, Yang X. Ultrasensitive Immunosensor for Cardiac Troponin I Detection Based on the Electrochemiluminescence of 2D Ru-MOF Nanosheets. Analytical Chemistry. 2019; 91(15): 10156-63.
33. Wang Y, Dostalek J, Knoll W. Long range surface plasmon-enhanced fluorescence spectroscopy for the detection of aflatoxin M1 in milk. Biosens. Bioelectron. 2009; 24: 2264-7.
34. Huang X, Yin Z, Wu S, Qi X, He Q, Zhang Q, et al. Graphen-Based Materials: Synthesis, Characterization, Properties, and Applications. Small. 2011; 14(7): 1876-902
35. Bai Y, Xu T, Zhang X. Graphene-based biosensors for detection of biomarkers. Micromachines. 2020; 11: 60.
36. Chekin F, Vasilescu A, Jijie R, Singh SK, Kurungot S, Iancu M, et al. Sensitive electrochemical detection of cardiac troponin I in serum and saliva by nitrogen-doped porous reduced graphene oxide electrode. Sensors Actuators B Chem. 2018; 262: 180-7.
37. Jo H, Gu H, Jeon W, Youn H, Her J, Kim SK, et al. Electrochemical aptasensor of cardiac troponin I for the early diagnosis of acute myocardial infarction, Anal. Chem. 2015; 87: 9869-75.
38. CHENG S. Detection of biomarkers using field effect transistor (FET)-based biosensors for disease diagnosis. 2015.
39. Ohno Y, Maehashi K, Matsumoto K. Label-Free Biosensors Based on Aptamer-Modified Graphene Field-Effect Transistors. J. Am. Chem. Soc. 2010; 132(51): 18012-3.
40. Kwong Hong D, sang T, et al. Chemically Functionalised Graphene FET Biosensor for the Label-free Sensing of Exosomes. Sci. Rep. 2019; 9(1): 211.
41. Szeto K, Craighead HG. Devices and approaches for generating specific high-affinity nucleic acid aptamers. Appl. Phys. Rev. 2014; 1: 031103.
42. Warszawski S, Borenstein Katz A, Lipsh R, et al. Optimizing antibody affinity and stability by the automated design of the variable light-heavy chain interfaces. PLoS Comput Biol. 2019; 15(8): e1007207.
43. Lakowicz, JR. Principles of Fluorescence Spectroscopy, Springer, 2006.
44. http://www.chemgapedia.de/vsengine/vlu/vsc/de/ch/13/vlu/kinetik/affinitaet/affinitaetsreaktionen.vlu/Page/vsc/de/ch/13/pc/kinetik/affinitaet/binkin.vscml.html.
45. Yao D, Yu F, Kim J, Scholz J, Nielsen PE, Sinner EK, Knoll W. Surface plasmon field-enhanced fluorescence spectroscopy in PCR product analysis by peptide nucleic acid probes. Nucleic Acids Research. 2004; 32: 22.

46. Stringer RC, Hoehn D, Grant SA. Quantum Dot-Based Biosensor for Detection of Human Cardiac Troponin I Using a Liquid-Core Waveguide. IEEE Sens. J. 2008; 8: 295-300.
47. Wu J, Cropek DM, West AC, Banta S. Development of a troponin I biosensorusing a peptide obtained through phage display, Anal. Chem. 2010; 82: 8235-43.
48. Sandil D, Kumar S, Arora K, Srivastava S, Malhotra B, Sharma S, Puri NK. Biofunctionalized nanostructured tungsten trioxide based sensor for cardiacbiomarker detection, Mater. Lett. 2017; 186: 202-5.
49. Guo ZR, Gu CR, Fan X, Bian ZP, Wu HF, Yang D, et al. Fabrication of Anti-human Cardiac Troponin I Immunogold Nanorods for Sensing Acute Myocardial Damage.Nanoscale Res. Lett. 2009; 4: 1428-33.
50. Kwon YC, Kim MG, Kim EM, Shin Y, Lee SK, Lee SD, et al. Development of a surface plasmon resonance-based immunosensorfor the rapid detection of cardiac troponin I, Biotechnol. Lett. 2011; 33: 921-7.
51. Torabi F, Mobini Far HR, Danielsson B, Khayyami M. Development of a plasma panel test for detection of human myocardial proteins by capillary immunoassay. Biosens Bioelectron. 2007; 22(7): 1218-23.
52. Dorraj GS, Rassaee MJ, Latifi AM, Pishgoo B, Tavallaei M. Selection of DNA aptamers against Human Cardiac Troponin I for colorimetric sensor based dot blot application. J. Biotechnol. 2015; 208: 80-6.
53. Pawula M, Altintas Z, Tothill IE. SPR detection of cardiac troponin T for acute myocardial infarction. Talanta. 2016; 146: 823-30.
54. Masson JF, Obando L, Beaudoin S, Booksh K. Sensitive and Real-Time Fiber-Optic-Based Surface Plasmon Resonance Sensors for Myoglobin and Cardiac Troponin I. Talanta. 2004; 62: 865-70.
55. Wu Q, Sun Y, Zhang D, et al. Ultrasensitive magnetic field-assisted surface plasmon resonance immunoassay for human cardiac troponin I. Biosens Bioelectron. 2017; 96: 288-93.
56. Jiang SH, Fan T, Liu LJ, Chen Y, Zhang XQ, Sha ZL, et al. The Detection of cTn I by The AptamerBiosensor. Progress in Biochemistry and Physics. 2014; 41: 916-20.
57. Ahammad AS, Choi YH, Koh K, Kim JH, Lee JJ, Lee M. Electrochemical detection of cardiac biomarker troponin I at gold nanoparticle-modified ITO electrode by using open circuit potential, Int. J. Electrochem. Sci. 2011; 6: 1906-16.
58. Jagadeesan KK, Kumar S, Sumana G. Application of conducting paper forselective detection of troponin, Electrochem. Commun. 2012; 20: 71-4.
59. Tan CM, Arshad MK, Fathil MFM, Adzhri R, Nuzaihan M, Ruslinda AR, et al. Interdigitated Electrodes Integrated with Zinc Oxide Nanoparticles for Cardiac Troponin I Biomarker Detection. IEEE-ICSE2016 Proc. 2016.
60. Gupta A, Sharma SK, Pachauri V, Ingebrandt S, Singh S, Sharma AL, et al. Sensitive impedimetric detection of troponin I with metal–organic framework composite electrode. RSC Advances. 2021; 11(4): 2167-74.
61. Mayilo S, Kloster MA, Wunderlich M, et al. Long-range fluorescence quenching by gold nanoparticles in a sandwich immunoassay for cardiac troponin T. Nano Lett. 2009; 9(12): 4558-63.
62. Zuo J, Zhao X, Ju X, Qiu S, Hu W, Fan T, et al. A new molecularly imprinted polymer (MIP)-based electrochemical sensor for monitoring cardiac troponin I (cTnI) in the serum, Electroanalysis 2016; 28: 2044-9.
63. Kiely J, Hawkins P, Wraith P, Luxton R. Paramagnetic Particle Detection for Use with an Immunoassay Based Biosensor. IETSci., Meas. Technol. 2007; 1: 270-5.
64. Bozdogan A, El-Kased RF, Jungbluth V, Knoll W, Dostalek J, Kasry A. Development of a specific troponin I detection system with enhanced immune sensitivity using a single monoclonal antibody. Royal Society Open Science. 2020; 7(10): 200871.
65. Periyakaruppan A, Gandhiraman RP, Meyyappan M, Koehne JE. Label-free detection of cardiac troponin-I using carbon nanofiber based nanoelectrode arrays, Anal. Chem. 2013; 85: 3858-63.
66. Silva BVM, Cavalcanti IT, Mattos AB, Moura P, Sotomayor MDPT, Dutra RF. Disposable immunosensor for human cardiac troponin Tbased on streptavidin-microsphere modified screen-printed electrode.Biosens Bioelectron. 2010; 26(3): 1062-7.
67. Bhalla V, Carrara S, Sharma P, Nangia Y, Suri CR. Gold nanoparticles-mediated label-free capacitance detection of cardiac troponin I, Sens. Actuators B. 2012; 161: 761-8.
68. Liu X, Wang Y, Chen P, McCadden A, Palaniappan A, Zhang J, et al. Peptide Functionalized Gold Nanoparticles with Optimized Particle Size and Concentration for Colorimetric Assay Development: Detection of Cardiac Troponin I. ACS Sens. 2016; 1(12): 1416-22.
69. Ko S, Kim B, Jo SS, Oh SY, Park JK. Electrochemical detection of cardiac troponin I using a microchip with the surface-functionalized poly(dimethylsiloxane) channel, Biosens. Bioelectron. 2007; 23: 51-9.
70. Jiang M-H, Lu P, Lei Y-M, Chai Y-Q, Yuan R, Zhuo Y. Selfaccelerated electrochemiluminescence emitters of Ag@SnO2 nanoflowers for sensitive detection of cardiac troponin T. Electrochim Acta. 2018; 271: 464-71.
71. Song SY, Han YD, Kim K, Yang SS, Yoon HC. A Fluoro-Microbead Guiding Chip for Simple and Quantifiable Immunoassay of Cardiac Troponin I (cTnI). Biosens. Bioelectron. 2011; 26: 3818-24.
72. Shumkov AA, Suprun EV, Shatinina SZ, Lisitsa AV, Shumyantseva VV, Archakov AI. Gold and silver nanoparticles for electrochemical detection ofcardiac troponin I based on stripping voltammetry. Bio-NanoScience. 2013; 3: 216-22.
73. Liu J, Zhang LL, Wang YS, Zheng Y, Sun S H. An improved portable biosensing system based on enzymatic chemiluminescence and magnetic immunoassay for biological compound detection. Measurement. 2014; 47: 200-6.
74. Zhang B, Morales AW, Peterson R, Tang L, Ye JY. Label-free Detection of Cardiac Troponin I with a Photonic Crystal Biosensor. Biosens. Bioelectron. 2014; 58: 107-13.
75. Lee KW, Kim KR, Chun HJ, Jeong KY, Hong DK, Lee KN, et al. Time-resolved fluorescence resonance energy transfer-based lateral flow immunoassay using a raspberry-type europium particle and a single membrane for the detection of cardiac troponin I. Biosensors and Bioelectronics. 2020; 163: 112284.
76. Kong T, Su R, Zhang B, Zhang Q, Cheng G. CMOS-compatible, label-freesilicon-nanowire biosensors to detect cardiac troponin I for acute

myocardialinfarction diagnosis, Biosens. Bioelectron. 2012; 34: 267-72.

77. Bruls DM, Evers TH, Kahlman JAH, van Lankvelt PJW, Ovsyanko M, Pelssers EGM, et al. Rapid Integrated Biosensor for Multiplexed Immunoassays Based on Actuated Magnetic Nanoparticles. Lab Chip. 2009; 9: 3504-10.

78. Kazemi SH, Ghodsi E, Abdollahi S, Nadri S. Porous graphene oxide nanostructure as an excellent scaffold for labelfree electrochemical biosensor: detection of cardiac troponin I. Mater Sci Eng C Mater Biol Appl. 2016; 69: 447-52.

79. Liu D, Lu X, Yang Y, Zhai Y, Zhang J, Li L. A novel fluorescent aptasensor for the highly sensitive and selective detection of cardiac troponin I based on a graphene oxide platform. Anal Bioanal Chem. 2018; 410(18): 4285-91.

80. Kwon YC, Kim MG, Kim EM, et al. Development of a surface plasmon resonance-based immunosensor for the rapid detection of cardiac troponin I. Biotechnol Lett. 2011; 33(5): 921-7.

81. Li F, Yu Y, Cui H, Yang D, Bian Z. Label-free electrochemiluminescence immunosensor for cardiac troponin I using luminol functionalized goldnanoparticles as a sensing platform. Analyst. 2013; 138: 1844-50.

82. Liu G, Qi M, Zhang Y, Cao C, Goldys EM. Nanocomposites of goldnanoparticles and graphene oxide towards an stable label-freeelectrochemical immunosensor for detection of cardiac marker troponin-I,Anal. Chim. Acta. 2016; 909: 1-8.

83. Vasantham S, Alhans R, Singhal C, Nagabooshanam S, Nissar S, Basu T, et al. Paper based point of care immunosensor for the impedimetric detection of cardiac troponin I biomarker. Biomedical Microdevices. 2020; 22(1).

84. Rezaei B, Shoushtari AM, Rabiee M, Uzun L, Mak WC, Turner APF. An electrochemical immunosensor for cardiac troponin, I using electrospun carboxylated multi-walled carbon nanotube -whiskered nanofibres. Talanta. 2018; 182: 178-6.

85. Dittmer WU, Evers TH, Hardeman WM, Huijnen W, Kamps R, de Kievit P, et al. Rapid, High Sensitivity, Point-Of-Care Test for Cardiac Troponin Based on Optomagnetic Biosensor. Clin. Chim. Acta. 2010; 411: 868-73.

86. Cho IH, Paek EH, Kim YK, Kim JH, Paek SH. Chemiluminometric Enzyme-Linked Immunosorbent Assays (ELISA)-on-a-Chip Biosensor Based on Cross-Flow Chromatography. Anal.Chim. Acta. 2009; 632: 247-55.

87. Horak J, Dincer C, Qelibari E, Bakirci H, Urban G. Polymer-modified microfluidic immunochip for enhanced electrochemical detection of troponinI, Sens. Act. 2015; 209: 478-85.

88. Jo H, Her J, Lee H, Shim YB, Ban C. Highly sensitive amperometric detection of cardiac troponin I using sandwich aptamers and screen-printed carbon electrodes. Talanta. 2017; 165: 442-8.

89. Lee T, Lee Y, Park SY, Hong K, Kim Y, Park C, et al. Fabrication of electrochemical biosensor composed of multi-functional DNA structure/Au nanospike on micro-gap/PCB system for detecting troponin I in human serum. Colloids Surf B Biointerfaces. 2019; 175: 343-50.

90. Qiao X, Li K, Xu J, Cheng N, Sheng Q, Cao W, et al. Novel electrochemical sensing platform for ultrasensitive detection of cardiac troponin I based on aptamer-MoS2 nanoconjugates. Biosens Bioelectron. 2018; 15; 113: 142-7.

91. Cai Y, Kang K, Li Q, Wang Y, He X. Rapid and sensitive detection of cardiac troponin I for point-of-care tests based on red fluorescent microspheres Molecules. 2018; 23: 1102.

92. Sun D, Luo Z, Lu J, Zhang S, Che T, Chen Z, Zhang L. Electrochemical dual-aptamer-based biosensor for nonenzymatic detection of cardiac troponin I by nanohybrid electrocatalysts labeling combined with DNA nanotetrahedron structure. Biosens Bioelectron. 2019; 134: 49-56.

93. Tu D, Holderby A, Coté GL. Aptamer-based surface-enhanced resonance Raman scattering assay on a paper fluidic platform for detection of cardiac troponin I. J. Biomed. Opt. 2020; 25(9): 097001.

94. Han X, Kojori HS, Leblanc RM, Kim SJ. Ultrasensitive Plasmonic Biosensors for Real-Time Parallel Detection of Alpha-L-Fucosidase and Cardiac-Troponin-I in Whole Human Blood. Analytical Chemistry. 2018; 90(13): 7795-9.

95. Peng J, Song G, Niu H, Wang P, Zhang X, Zhang S, Chen D. Detection of cardiac biomarkers in serum using a micro-electromechanical film electroacoustic resonator. Journal of Micromechanics and Microengineering. 2020; 30(7): 075011.

96. Bruls DM, Evers TH, Kahlman JAH, et al. Rapid integrated biosensor for multiplexed immunoassays based on actuated magnetic nanoparticles.Lab Chip. 2009; 9(24): 3504-10.

97. Cho IH, Paek EH, Kim YK, Kim JH, Paek SH. Chemiluminometric enzyme-linked immunosorbent assays (ELISA)-on-a-chip biosensor based on cross-flow chromatography. Anal Chim Acta. 2009; 632(2): 247-55.

98. Choi DH, Lee SK, Oh YK, Bae BW, Lee SD, Kim S, et al. A Dual Gold Nanoparticle Conjugate-BasedLateral Flow Assay (LFA) Method for the Analysis of Troponin I.Biosens. Bioelectron. 2010; 25: 1999-2002.

99. Wu WY, Bian ZP, Wang W, Zhu JJ. PDMS gold nanoparticle compositefilm-based silver enhanced colorimetric detection of cardiac troponin I, Sens.Actuators B. 2010; 147: 298-303.

100. Rajesh, Sharma V, Puri NK, Singh RK, Biradar RM, Mulchanadani A. Label-free detection of cardiac troponin-I using gold nanoparticles functionalized single-walled carbon nanotubes based chemiresistive biosensor. Appl. Phys. Lett. 2013; 103: 203703.

101. Pedrero M, Campuzano S, Pingarrón JM. Electrochemical biosensors for the determination of cardiovascular markers: a review. Electroanalysis. 2014; 26(6): 1132-53.

102. Sandil D, Srivastava S, Malhotra B, Sharma S, Puri NK. Biofunctionalized tungsten trioxide-reduced graphene oxide nanocomposites for sensitive electrochemical immunosensing of cardiac biomarker. J Alloys Compd. 2018; 763: 102-10.

103. Negahdary M, Behjati-Ardakani M, Sattarahmady N, Yadegari H, Heli H. Electrochemical aptasensing of human cardiac troponin I based on an array of gold nanodumbbells-Applied to early detection of myocardialinfarction, Sensors and Actuators B: Chemical. 2017; 252: 62-71.

104. Yen PW, Huang CW, Huang YJ, Chen MC, Liao HH, Lu SS, et al. A device design of an integrated CMOS poly-silicon biosensor-on-chip

to enhance performance of biomolecular analytes in serum samples. Biosens. Bioelectron. 2014; 61: 112-8.

105. Shen SH, Wang IS, Cheng H, Lin CT. An enhancement of high-k/ oxide stacked dielectric structure for silicon-based multi-nanowire biosensor in cardiac troponin I detection. Sens. Act. 2015; 218: 303-9.

106. Sun D, Lin X, Lu J, Wei P, Luo Z, Lu X, Chen Z, Zhang L. DNA nanotetrahedron-assisted electrochemical aptasensor for cardiac troponin I detection based on the co-catalysis of hybrid nanozyme, natural enzyme and artificial DNAzyme. Biosens Bioelectron. 2019; 142.

107. Lee J, Lee Y, Park JY, Seo H, Lee T, Lee W, et al. Sensitive and reproducible detection of cardiactroponin I in human plasma using a surface acoustic wave immunosensor,Sens. Actuators. 2013; 178: 19-25.

108. Sarangadharana I, Regmia A, Chena YW, Hsua CP, Chena PC, Changb WH, et al. High sensitivity cardiac troponin I detection in physiological environment using AlGaN/GaN High Electron Mobility Transistor (HEMT) Biosensors. Biosens. Biolelectron. 2018; 100: 282-9.

109. Yan H, Tang X, Zhu X, Zeng Y, Lu X, Yin Z, et al. Sandwich-type electrochemical immunosensor for highly sensitive determination of cardiac troponin I using carboxylterminated ionic liquid and helical carbon nanotube composite as platform and ferrocenecarboxylic acid as signal label. Sensors Actuators B Chem. 2018; 277: 234-40.

110. Luo Z, Sun D, Tong Y, Zhong Y, Chen Z. DNA nanotetrahedron linked dual-aptamer based voltammetric aptasensor for cardiac troponin I using a magnetic metal-organic framework as a label. Mikrochim Acta. 2019; 186(6): 374.

111. Wang Y, Yang Y, Chen C, Wang S, Wang H, Jing W, et al. One-Step Digital Immunoassay for Rapid and Sensitive Detection of Cardiac Troponin I. ACS Sensors. 2020; 5(4): 1126-31.

112. Wu M, Zhang X, Wu R, Wang G, Li G, Chai Y, et al. Sensitive and Quantitative Determination of Cardiac Troponin I Based on Silica-Encapsulated CdSe/ZnS Quantum Dots and a Fluorescence Lateral Flow Immunoassay. Analytical Letters. 2020; 53(11) 1757-73.

113. Aslan K, Grell TA. Rapid and Sensitive Detection of Troponin I in Human Whole Blood Samples by Using Silver Nanoparticle Films and Microwave Heating. Clin. Chem. 2011; 57: 746-52.

114. Fu X, Wang Y, Liu Y, Liu H, Fu L, Wen J, et al. A graphene oxide/gold nanoparticle-based amplification method for SERS immunoassay of cardiac troponin I. Analyst. 2019; 144: 1582-9.

115. Kim K, Park C, Kwon D, Kim D, Meyyappan M, Jeon S, Lee JS. Silicon nanowire biosensors for detection of cardiac troponin I (cTnI) with high sensitivity, Biosens. Bioelectron. 2016; 77: 695-701.

116. Lopa NS, Rahman MM, Ahmed F, Ryu T, Sutradhar SC, Lei J, et al. Simple, low-cost, sensitive and label-free aptasensor for the detection of cardiac troponin I based on a gold nanoparticles modified titanium foil. Biosens Bioelectron. 2019; 126: 381-8.

117. Singal S, Srivastava AK, Biradar AM, Mulchandani A. Ptnanoparticles-chemical vapor deposited graphene composite basedimmunosensor for the detection of human cardiac troponin I, Sens. ActuatorsB. 2014; 205: 363-70.

118. Zhou F, Lu M, Wang W, Bian ZP, Zhang JR, Zhu JJ. Electrochemical Immunosensor for Simultaneous Detection of Dual Cardiac Markers Based on a Poly(Dimethylsiloxane)-Gold Nanoparticles Composite Microfluidic Chip: A Proof of Principle. Clin. Chem. 2010; 56: 1701-7.

119. Wang B, Jing R, Qi H, Gao Q, Zhang C. Label-free electrochemical impedancepeptide-based biosensor for the detection of cardiac troponin I incorporatinggold nanoparticles modified carbon electrode, J. Electroanal. Chem. 2016; 781: 212-7.

120. Fathil MFM, Md Arshad MK, Ruslinda AR, Gopinath SBC, Nuzaihan M, Adzhri MNR, et al. Substrate-gate coupling in ZnO-FETbiosensor for cardiac troponin I detection, Sens. Actuators. 2017; 242: 1142-54.

121. Wang B, Jing R, Qi H, Gao Q, Zhang C. Label-free electrochemical impedance peptide-based biosensor for the detection of cardiac troponin I incorporating gold nanoparticles modified carbon electrode. J Electroanal Chem. 2016; 78: 212-7.

122. Park JP, Cropek DM, Banta S. High affinity peptides for the recognition of the heart disease biomarker troponin I identified using phage display.Biotechnol Bioeng. 2010; 105(4): 678-86.

123. Shen W, Tian D, Cui H, Yang D, Bian Z. Nanoparticle-basedelectrochemiluminescence immunosensor with enhanced sensitivity forcardiac troponin I using N-(aminobutyl)-N-(ethylisoluminol)-functionalizedgold nanoparticles as labels, Biosens. Bioelectron. 2011; 27: 18-24.

124. Jarvenpaa ML, Kuningas K, Niemi I, Hedberg P, Ristiniemi N, Pettersson K, et al. Rapid and Sensitive Cardiac Troponin I Immunoassay Based on Fluorescent Europium(III)-Chelate-Dyed Nanoparticles. Clin. Chim. Acta. 2012; 414: 70-5.

125. Tuteja K, Priyanka SK, Bhalla V, Deep A, Paul AK, Suri CR. Graphene-gated biochip for the detection of cardiac marker Troponin I. Anal. Chim. Acta. 2014; 809: 148-54.

126. Tuteja SK, Sabherwal P, Deep A, Rastogi R, Paul AK, Suri CR. Biofunctionalized rebar graphene (f-RG) for label free detection of cardiac marker troponin I. ACS Appl. Mat Interfaces. 2014; 6(17): 14767-71.

127. Singal S, Srivastava AK, Gahtori B, Rajesh. Immunoassay for troponin I using a glassy carbon electrode modified with a hybrid film consisting of graphene and multiwalled carbon nanotubes and decorated with platinum nanoparticles. Microchim Acta. 2016; 183(4): 1-10.

128. Shanmugama NR, Muthukumarb S, Chaudhry S, Anguianao J, Prasad S. Ultrasensitive nanostructure sensor arrays on flexible substrates for multiplexed and simultaneous electrochemical detection of a panel of cardiac biomarkers. Biosens Bioelectron. 2017; 89: 764-72.

129. Grabowska I, Sharma N, Vasilescu A, Iancu M, Badea G, Boukherroub R, et al. Electrochemical Aptamer-Based Biosensors for the Detection of Cardiac Biomarkers. ACS Omega. 2018; 3(9): 12010-8.

130. Singal S, Srivastava AK, Dhakate S, Biradar AM, Rajesh R. Electroactive graphene-multi-walled carbon nanotube hybrid supported impedimetric immunosensor for the detection of human cardiac troponin-I. RSC Adv 2015; 5(92): 74994-5003.

131. Han GR, Ki H, Kim MG. Automated, Universal, and Mass-Producible Paper-Based Lateral Flow Biosensing Platform for High-Performance Point-of-Care Testing. ACS Applied Materials & Interfaces. 2020; 12(1) 1885-94.

132. Dong M, Li M, Qi H, Li Z, Gao Q, Zhang C. Electrogeneratedchemiluminescence peptide-based biosensing method for cardiac troponin

Iusing peptide-integrating Ru (bpy) 3 2+-functionalized gold nanoparticles asnanoprobe, Gold Bull. 2015; 48: 21-9.

133. Saremi M, Amini A, Heydari H. An aptasensor for troponin I based on the aggregation-induced electrochemiluminescence of nanoparticles prepared from a cyclometallated iridium(III) complex and poly(4-vinylpyridine-co-styrene) deposited on nitrogen-doped graphene. Mikrochim Acta. 2019 22; 186(4): 254.

134. Shan M, Li M, Qiu XY, Qi HL, Gao Q, Zhang CX. Sensitive Electrogenerated Chemiluminescence Peptide-based Biosensor for the Determination of Troponin I with Gold Nanoparticles Amplification. Gold Bull. 2014; 47: 57-64.

135. Lee I, Luo X, Huang J, Cui XT, Yun M. Detection of Cardiac Biomarkers Using Single Polyaniline Nanowire-Based Conductometric Biosensors. Biosens. 2012; 2: 205-20.

136. Todd J, Freese B, Lu A, Held D, Morey J, Livingston R, et al. Ultrasensitive Flow-Based Immunoassays Using Single-Molecule Counting. Clin. Chem. 2007; 53: 1990-5.

137. Zhang T, Ma N, Ali A, Wei Q, Wu D, Ren X. Electrochemical ultrasensitive detection of cardiac troponin I using covalent organic frameworks for signal amplification. Biosens Bioelectron. 2018; 119: 176-81.

138. Çimen D, Bereli N, Günaydın S, Denizli A. Detection of cardiac troponin-I by optic biosensors with immobilized anti-cardiac troponin-I monoclonal antibody. Talanta. 2020; 219: 121259.

139. Kar P, Pandey A, Greer JJ, Shankar K. Ultrahigh Sensitivity Assays for Human Cardiac Troponin I Using TiO2 Nanotube Arrays. Lab Chip. 2012; 12: 821-8.

140. Mi X, Li H, Tan R, Tu Y. Dual-Modular Aptasensor for Detection of Cardiac Troponin I Based on Mesoporous Silica Films by Electrochemiluminescence/Electrochemical Impedance Spectroscopy. Analytical Chemistry 2020; 92(21): 14640-7.

141. Lv H, Zhang X, Li Y, Ren Y, Zhang C, Wang P, et al. An electrochemical sandwich immunosensor for cardiac troponin I by using nitrogen/sulfur co-doped graphene oxide modified with Au@Ag nanocubes as amplifiers. Mikrochim Acta. 2019; 186(7): 416.

142. Xu Z, Dong Y, Li J, Yuan R. A ferrocene-switched electro-chemiluminescence „off-on" strategy for the sensitive detection of cardiac troponin I based on target transduction and a DNA walking machine. Chem Commun (Camb). 2015; 51(76): 14369-72.

143. Zhang L, Xiong C, Wang H, Yuan R, Chai Y. A sensitiveelectrochemiluminescence immunosensor for cardiac troponin I detection based on dual quenching of the self-enhanced Ru(II) complex by folic acid andin situ generated oxygen, Sens. Actuators B. 2017; 241: 765-72.

144. Akanda MR, Aziz MA, Jo K, Tamilavan V, Hyun MH, Kim S, Yang H. Optimization of phosphatase-and redox cycling-based immunosensors and its application to ultrasensitive detection of troponin I, Anal. Chem. 2011; 83: 3926-33.